Available online at www.sciencedirect.com
SCIENCE DIRECT
Thermochimica Acta 444 (2006) 179–189
thermochimica acta
www.elsevier.com/locate/tca

Determination of carbonation profiles in non-hydraulic lime mortars using thermogravimetric analysis

R.M.H. Lawrence [a], T.J. Mays [b,*], P. Walker [a], D. D'Ayala [a]

[a] *Department of Architecture and Civil Engineering, University of Bath BA2 7AY, United Kingdom*
[b] *Department of Chemical Engineering, University of Bath BA2 7AY, United Kingdom*

Received 19 December 2005; received in revised form 15 February 2006; accepted 2 March 2006
Available online 24 April 2006

Abstract

The carbonation profile of material taken at various depths in a lime mortar specimen has been determined at different times from manufacture using a novel, high-speed thermogravimetric analysis (TGA) method. While conventional phenolphthalein staining suggests a sharp boundary between carbonated and non-carbonated regions, the new TGA technique shows that up to 15% (w/w) of portlandite remains uncarbonated at the exterior of the mortar and that the extent of carbonation declines linearly over up to 15 mm into the interior. The technique demonstrates the possibility of identifying the presence of Liesegang patterns by measuring variations in the concentration of $Ca(OH)_2$ through the depth profile.

Keywords: Non-hydraulic lime mortar; Air lime; TGA; Carbonation profile; Liesegang patterns

1. Introduction

In the field of conservation and restoration of the historic built environment, it has been shown that the use of cement based mortars in repair and restoration causes rapid and significant deterioration to the historic substrate [1]. This deterioration is caused by the incompatibility of excessively hard and impervious cementitious mortars with weaker and more porous historic stone and brick. The use of non-hydraulic and feebly hydraulic lime mortars avoids these difficulties.

By the latter half of the 20th century lime mortars had become rarely used and poorly understood in construction. However, their evident value in restoring historic buildings requires that their properties are well characterised so that suitable formulations can be made for specific purposes.

Hydraulic lime mortars set partly through the well-understood process of metal oxide hydration that takes place in cement and partly through the less well-understood process of carbonation. Non-hydraulic lime mortars set entirely through carbonation. Carbonation is the process whereby slaked lime, or portlandite ($Ca(OH)_2$) reacts with atmospheric carbon dioxide (CO_2) to form the significantly stronger and less soluble calcium carbonate, or calcite ($CaCO_3$). For carbonation to occur, the presence of water is essential, since it requires the dissolution of CO_2. $Ca(OH)_2$ is accessed by the CO_2 in its dissolved state [2]. There are five stages involved:

1. diffusion of gaseous CO_2 through the pores of the mortar;
2. dissolution of the CO_2 in the pore water;
3. dissolution of $Ca(OH)_2$ in the pore water;
4. chemical equilibration of dissolved CO_2 in the pore water;
5. precipitation of $CaCO_3$.

The influence of the amount of mixing water used is therefore significant, since this will affect the pore structure of the hardened mortar [3].

Although a wide range of methods is available to measure carbonation [4], the traditional method of detecting this process is to spray a freshly broken surface of mortar with phenolphthalein. Where the surface is stained deep red it indicates the presence of the highly alkaline portlandite, whereas uncoloured areas indicate that the portlandite has carbonated into neutral calcite. The implication often drawn from this is that there is a sharp boundary between carbonated and uncarbonated material. It has, however, been demonstrated that a carbonation front develops which moves through the material as carbonation progresses

* Corresponding author. Tel.: +44 1225 386528; fax: +44 1225 385713.
E-mail address: t.j.mays@bath.ac.uk (T.J. Mays).

0040-6031/$ – see front matter © 2006 Elsevier B.V. All rights reserved.
doi:10.1016/j.tca.2006.03.002

Table 1
Filler density and water absorption characteristics and water required to produce a given flow value as calculated using BS 1097-6

	Sand	Bioclastic stone	Oolitic stone
Apparent particle density (Mg/m^3)	2.77	2.67	2.54
Particle density on an oven dried basis (Mg/m^3)	2.76	2.30	2.21
Particle density on a saturated and surface dried basis (Mg/m^3)	2.76	2.44	2.34
Water absorption (%)	0.1	6.1	5.9
Water/lime ratio required to make 25–30% flow (v/v)	1.07	1.15	1.12
'Free' water/lime ratio (v/v)	1.07	1.08	1.05

[5]. Until now no satisfactory technique has been available to measure the shape of this front.

This paper builds on earlier work [6] that demonstrated how a new thermogravimetric analysis (TGA) method might be used to determine the extent of carbonation in lime mortars. The aim is to show how this method may be applied to measure the amount of portlandite present at different distances from the surface of the mortar at different time intervals from manufacture. These measurements allow the carbonation front to be mapped in detail and as a result an insight can be gained into the kinetics of the carbonation process.

The value of this work stems from the fact that in non-hydraulic lime mortars, the carbonation process is largely responsible for their strength gain over time. The rate at which carbonation occurs and the shape of the carbonation front will therefore have a significant effect on the development of performance of such mortars. The ability to measure these changes will contribute to the understanding of how different mortars will develop over time, and therefore assist in the design of a particular mortar for a particular purpose.

Most importantly, the technique described in this paper uses very small quantities of material and can be used to test mortars in situ on the building causing minimal damage in a way that phenolphthalein staining could not achieve. Testing of lime mortars in situ over extended time periods allows researchers and practitioners to monitor the progress of carbonation and provides early warning of problems which could be associated with poor workmanship or quality control in manufacture.

2. Experimental

2.1. Materials

Lime mortar samples, typical of those used in building restoration, were manufactured using one part of 4 month-old slaked lime putty and three parts of three different fillers: crushed bioclastic stone, crushed oolitic stone and silicate sand. The proportions were on the basis of dry volumes of portlandite and filler, thus the amount of lime putty added to the mix was that which, when dried, would have comprised 25% of the total volume of dry ingredients.

The mortars under test were made using a paddle mixer and the workability of each mix was controlled since the intention was to work with mortars, which could be used for plastic repairs. These require a stiff texture similar to modelling clay. Where necessary, water was added to the mixes to produce a flow as measured on a flow table [7] of between 125 and 130 mm. The water/lime ratio was calculated using the amount of water present in the lime putty plus any additional water added during the mixing process.

The amount of water required to achieve a given flow varied according to the type of filler used. This was a function of the water absorption characteristics of the fillers. Table 1 gives the water requirements for each filler as well as particle density and water absorption as calculated using BS 1097-6 (units used are as specified in the standard).

In cement-based materials, the ratio of cement to mixing water has the most significant influence on the compressive strength of a mortar [8]. This relationship is also evident, but to a less marked extent, with hydraulic lime mortars [9]. The impact of the water/lime ratio on the compressive strength of non-hydraulic lime mortars is less well understood, and the authors are undertaking a series of tests to clarify this matter. In the case of cement the higher porosity produced by excess mixing water results in lower strengths. However, in the case of non-hydraulic lime mortars previous work has shown that higher porosity can in fact result in higher strength by offering greater access to CO_2 and hence better carbonation [10,11]. It has been shown that the porosity of lime pastes increases with an increase in the water/lime ratio [3]. An increase in porosity will improve the access of CO_2 to the interior of the mortar, and therefore impact on the rate of carbonation. Above a critical limit, excess water tends to cause shrinkage cracks, which result in a weaker mortar. In the case of these mortars the 'free' water/lime ratio varied between 1.05 and 1.08.

Mortars were cast in plywood moulds similar to those used by the Smeaton Project [12], but in the smaller dimensions of 50 mm × 50 mm × 250 mm. The moulds were lined with a breathable membrane (Tyvek®) to facilitate de-moulding while allowing the passage of moisture and gases in order not to inhibit carbonation. De-moulding took place 5 days after casting. Curing followed BSEN 1015-11:1999 [13] with 7 days at ∼90% RH, and subsequently at 60% RH and 20 °C until testing. Carbon dioxide levels were monitored, and were found to be ∼290 parts per million (ppm), which is the normal atmospheric concentration, except when specimens were being collected for testing, when levels increased to ∼350 ppm.

2.2. Sampling

There is no standardised time-frame for the testing of non-hydraulic lime mortars. Lanas and Alvarez-Galindo [10] used 3, 7, 28, 91, 182 and 365 days; Bromblet [14] used 7, 28, 90 and

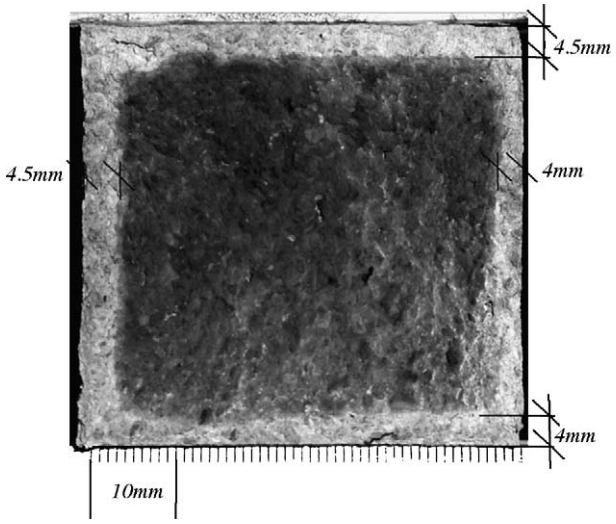

Fig. 1. Phenolphthalein staining on a 28 day-old lime mortar specimen.

120 days; Stewart et al. [15] used 60 and 120 days; Baronio et al. [16] used 28, 90, 180, 360 and 720 days. The choice of the starting time for the current experiments was based on the fact that the carbonation process can only begin once excess pore blocking water has evaporated, and hence very little carbonation is likely to occur before 14 days. Subsequent time intervals follow the traditional time intervals. This study used intervals of 14, 28, 90 and 180 days from manufacture. At each time interval a specimen was split transversely with a bolster.

The freshly broken surface was sprayed with phenolphthalein and photographed alongside a scale rule (Fig. 1).

The broken face was then sawn parallel to the fracture surface to produce a plane section through the mortar. Samples of ~150 μl were taken using a converted 5 mm diameter router at 3 mm intervals (5 mm for early tests, and 0.67 mm for more detailed tests) through the material until a depth of 24 mm was achieved (Fig. 2). The maximum particle size of fillers was 2 mm (8 μl or 5% of the sample size) and their granulometry is as described in Fig. 3.

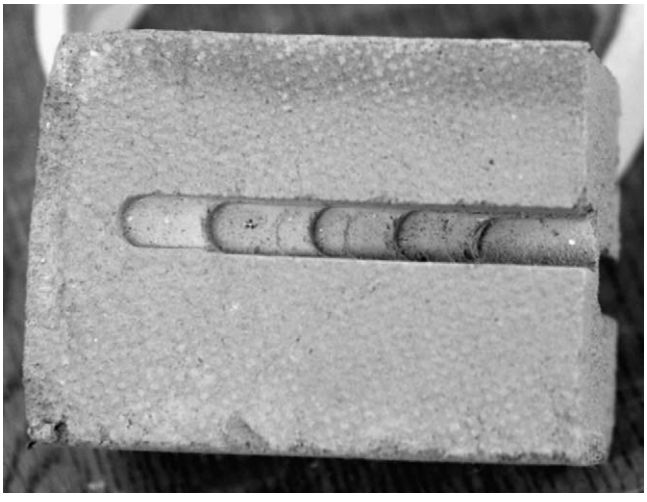

Fig. 2. Illustration of depth profiles taken with a router in a 50 mm wide specimen. (NB in practice each profile is taken directly on top of the previous one.)

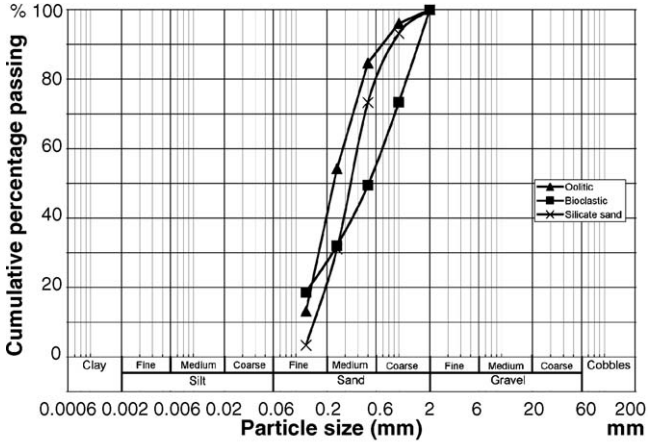

Fig. 3. Granulometry of fillers in lime mortar specimens.

These samples were then ground with an agate pestle and mortar to ~60 μm before being placed in separate universal bottles in a vacuum desiccator for 24 h. The bottles were then filled with nitrogen and sealed. This was done in order to avoid the carbonation process continuing [17]. TGA was also carried out on a freshly made sample of each mix of mortar to establish a base line for the amount of portlandite originally present.

2.3. TG testing

Thermogravimetry is a technique which produces very precise data on the quantities of $Ca(OH)_2$ and $CaCO_3$ present in a sample of lime mortar. The thermal breakdown of a non-hydraulic lime is a very simple and well-differentiated two part process. $Ca(OH)_2$ loses its chemically bound water between 350 and 550 °C (dehydroxylation) and $CaCO_3$ loses its chemically bound CO_2 between 600 and 900 °C (decarboxylation). The mortar mix of the specimen was designed in such a way that, within the dehydroxylation temperature range, none of the materials in the fillers show any thermal decomposition. The temperature range within which thermal decomposition can be seen within the fillers is between 100 and 330 °C, due to the

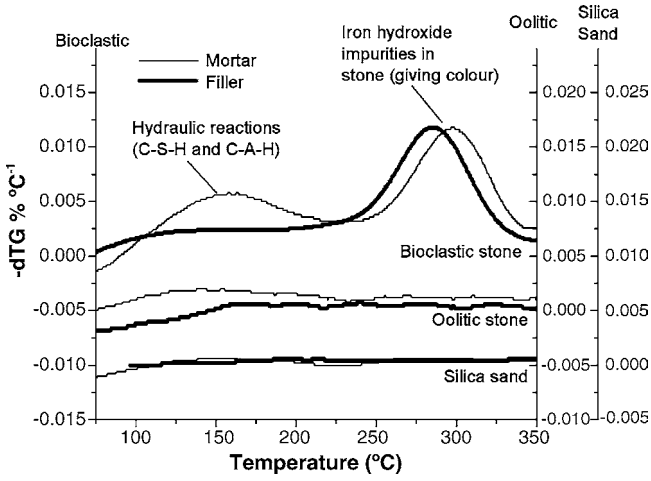

Fig. 4. dTG curves for all three filler types and 28 day-old filler:lime mortars.

presence of impurities, particularly in the bioclastic filler. The impurities within this filler consist of goethite which decomposes between 225 and 330 °C [18]. This impurity also has pozzolanic characteristics which produce thermal decomposition between 110 and 225 °C when mixed with lime and hydrated. These decompositions can be seen in Fig. 4. No further thermal decomposition is seen in any of the fillers until ∼600 °C, at which point the $CaCO_3$ present in the crushed stone fillers decomposes into CaO and CO_2 up to ∼900 °C.

Testing was conducted using a refurbished Setaram TGA 92 thermogravimetric analyser. Approximately 50 mg (∼40 μl) of material was heated in an alumina crucible in dry flowing air (16 cm^{-3} [STP] min^{-1}), at 50 °C min^{-1} to 650 °C. This heating rate has previously been demonstrated to produce accurate results within an acceptable time-frame [6]. Each data point was the result of one test. Since the mortar under test is relatively homogeneous, and ∼30% of the sample was tested, results can be considered to be representative of a bulk analysis at each depth through the material. This assumption has been verified by repeating tests three times on the same sample at three different $Ca(OH)_2$ concentrations. The maximum variation between results was found to be 3%. This potential error has been shown in the graphical representations of the carbonation front as an error bar on the *Y*-axis.

2.4. Treatment of TGA data

The first derivative of the TG data (dTG data) was calculated using a centred difference numerical differentiation formula. Inspection of the dTG data allows the start and end temperatures of the dehydroxylation process to be easily identified. Fig. 5 shows typical data at very low concentrations of $Ca(OH)_2$.

The measured weight loss during dehydroxylation is the chemically bound water which is given off as a vapour. Hence, from the reaction stoichiometry, the measured weight loss can be used to calculate the weight of $Ca(OH)_2$ originally present. Thus each milligram of weight loss results from the thermal decomposition of 74/18 = 4.111 mg of $Ca(OH)_2$. The weight loss between the two temperatures of 443 and 558 °C, can be determined from the dTG curve shown in Fig. 5. In this case the weight measured represents 0.50% of the specimen, which means that the specimen contained 2.06 wt.% portlandite. In this case the freshly made mortar contained 11.47 wt.% portlandite. Thus 82.1 wt.% of the portlandite in this sample can be shown to have carbonated. For each time and depth interval the raw TG data were converted using stoichiometry into percentage carbonation data and presented graphically in order to map the carbonation front.

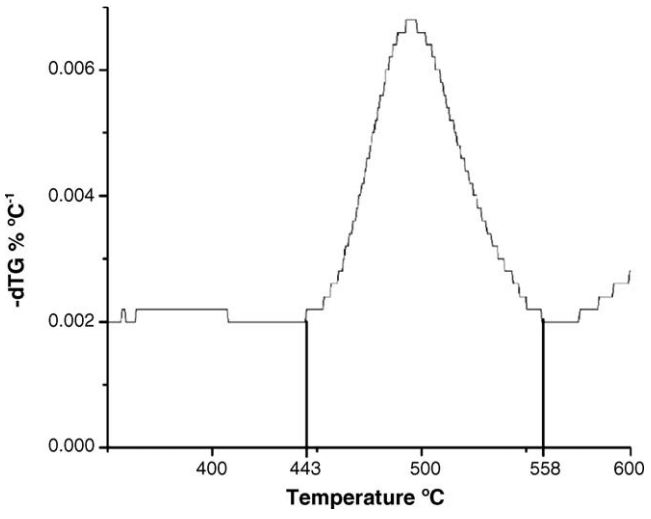

Fig. 5. dTG curve for the exterior 3 mm of a 90 day-old lime mortar made with oolitic fillers between 350 and 600 °C.

3. Results

The percentage $Ca(OH)_2$ at each depth interval calculated from the raw TG data using the stoichiometry as described above is presented in Table 2 in columns 2–5. The percentage carbonation deduced to have been achieved at each depth interval is given in columns 6–9. This has been calculated by comparing the percentage $Ca(OH)_2$ found at each depth interval with that found in freshly manufactured material. The difference is considered to be the amount of $Ca(OH)_2$ which has carbonated. In addition, at each time interval, the depth of material which is unstained by phenolphthalein is given (phenolphthalein carbonation depth). These depths have been measured by placing an image of a phenolphthalein stained specimen (Fig. 1) in a CAD programme. The image is then scaled to 1:1 by reference to the scale rule on the image. It is then possible to measure the depth of carbonation with great accuracy on each face. The average of the four measurements can then be used as the carbonation depth. This is the conventional method used by researchers and practitioners to assess the extent of carbonation.

At the start of the experimental series, sampling was taken at 5 mm depth intervals. This was subsequently reduced to 3 mm intervals for better resolution. It is considered quite practical to reduce this interval still further to 2 mm or even 1 mm depending on the maximum grain size of the filler. The accuracy of the data would be compromised by sampling intervals much smaller than the maximum filler grain size since there would be a risk that the sample would then contain an unrepresentatively high proportion of filler compared with binder. Under these circumstances the TGA data would tend to overestimate the extent of carbonation.

The ‘average 0–25 mm’ measurements shown in Table 2 are made on a sample of ∼150 μl taken using the router bit set at 25 mm depth. Thus the material sampled represents a cross-section of the depth of the specimen from the exterior to the core.

In order to visualise the carbonation front, the data in Table 2 are presented graphically in Figs. 6–9. Each figure shows data for one mortar type. The percentage carbonation curves at each time interval illustrate the carbonation front and its progression through the depth of the material. For ease of interpretation, the data points have been joined by straight lines to approximately describe the carbonation front. Superimposed on these are vertical lines which represent the depth of carbonation as measured by phenolphthalein staining. Error bars have been shown to one

Table 2
Calculated $Ca(OH)_2$ and carbonation percentages for three lime mortars over 90 days

Sample depth from-to (mm)	$Ca(OH)_2$ calculated from TGA data (wt.%)				Carbonation (%)			
	Day 14	Day 28	Day 90	Day 180	Day 14	Day 28	Day 90	Day 180
One part 4 month old lime putty: three parts crushed oolitic stone (11.62 wt.% $Ca(OH)_2$ when manufactured)								
Phenolphthalein carbonation depth (mm)					2.5	4.5	9.0	15.5
Average 0–25	10.67	9.13	7.28	6.17	8.18	21.43	37.35	46.90
0–5	2.75	2.14			76.33	81.58		
0–3			2.06	2.34			82.27	79.86
3–6			2.1	2.14			81.93	81.58
5–10	10.73	8.69			7.66	25.22		
6–9			2.01	2.67			82.70	77.02
9–12			8.47	3			27.11	74.18
10–15	10.77	9.37			7.31	19.36		
12–15			9	2.55			22.55	78.06
15–18			9.62	9.8			17.21	15.66
15–20	11.15	10.73			4.04	7.66		
18–21			9.7	9.78			16.52	15.83
20–25	11.47	11.31			1.29	2.67		
21–24			9.33	10.36			19.71	10.84
One part 4 month old lime putty: three parts silicate sand (6.80 wt.% $Ca(OH)_2$ when manufactured)								
Phenolphthalein carbonation depth (mm)					3.0	6.5	14.5	n/a
Average 0–25	6.58	4.25	2.84	0.58	36.97	59.29	72.80	91.54
0–3	0.86	1.09	0.78	0.58	87.35	83.97	88.53	91.54
3–6	3.65	2.43	0.86	0.66	46.32	64.26	87.35	90.33
6–9	4.34	3.25	0.99	0.86	36.18	52.21	85.44	87.30
9–12	3.82	4.07	0.74	0.66	43.82	40.15	89.12	90.33
12–15	4.32	4.89	1.4	0.58	36.47	28.09	79.41	91.54
15–18	5.36	4.77	2.8	0.58	21.18	29.85	58.82	91.54
18–21	6.31	4.06	3.58	0.53	7.21	40.29	47.35	92.14
21–24	6.8	5.02	3.54	0.58	0.00	26.18	47.94	91.54
One part 4 month old lime putty: three parts crushed bioclastic stone (10.94 wt.% $Ca(OH)_2$ when manufactured)								
Phenolphthalein carbonation depth (mm)					2.5	4.5	9.0	16.5
Average 0–25	8.39	8.14	7.85	4.07	23.31	25.59	28.24	62.80
0–5	7.51	3.82			31.35	65.08		
0–3			1.89	1.4			82.72	87.20
3–6			2.01	1.48			81.63	86.47
5–10	8.39	8.14			23.31	25.59		
6–9			1.89	1.56			82.72	85.74
9–12			7.61	1.59			30.44	85.47
10–15	8.84	9.21			19.20	15.81		
12–15			8.3	1.52			24.13	86.11
15–18			9.02	3.7			17.55	66.18
15–20	9.17	8.75			16.18	20.02		
18–21			9.17	5.47			16.18	50.00
20–25	9.33	8.67			14.72	20.75		
21–24			9.11	6.02			16.73	44.97

side for clarity: ±2.5 mm in the *X*-axis for the early tests and ±1.5 mm in the *X*-axis for the later tests with ±3% (absolute) in the *Y*-axis.

The carbonation front can be seen to progress through the depth of the material with a slope which varies in steepness between the relatively steep front for oolitic mortar and much more shallow one for sand mortar. The shape of the slope is a function of the permeability of the mortar to CO_2 and the amount of water present in the pores. One common feature that can be distinguished is that the core of each of the mortars is carbonating, but at a slower rate than the exterior. This indicates that low concentrations of CO_2 are available throughout the curing process ahead of the carbonation front. The extent of this also appears to be a function of the pore size distribution of the mortar since the sand mortar shows the greatest core carbonation. The open porosity of each mortar type was calculated using BSEN 1936 [19] and is shown in Table 3 below:

The pore size distribution as measured by Mercury Intrusion Porosimetry is as shown in Table 4. 29.17% of the pores in the silicate sand mortar are larger than 10 μm, compared with 13.33% of the bioclastic and 2.88% of the oolitic. It is these larger pores which offer the greatest access to atmospheric CO_2. The

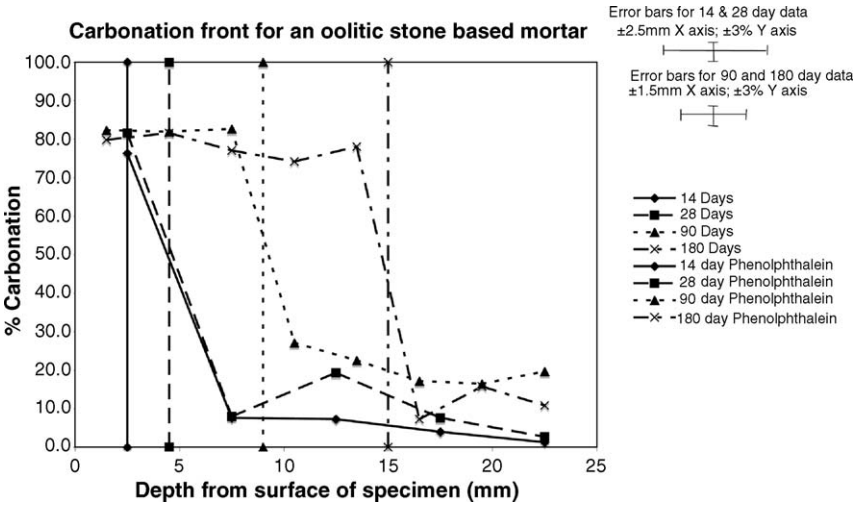

Fig. 6. Carbonation calculations for a lime mortar made with crushed oolitic stone.

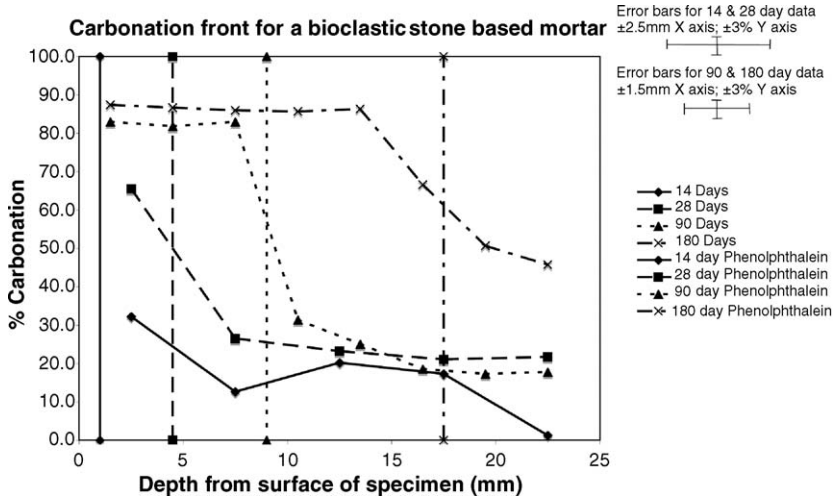

Fig. 7. Carbonation calculations for a lime mortar made with crushed bioclastic stone.

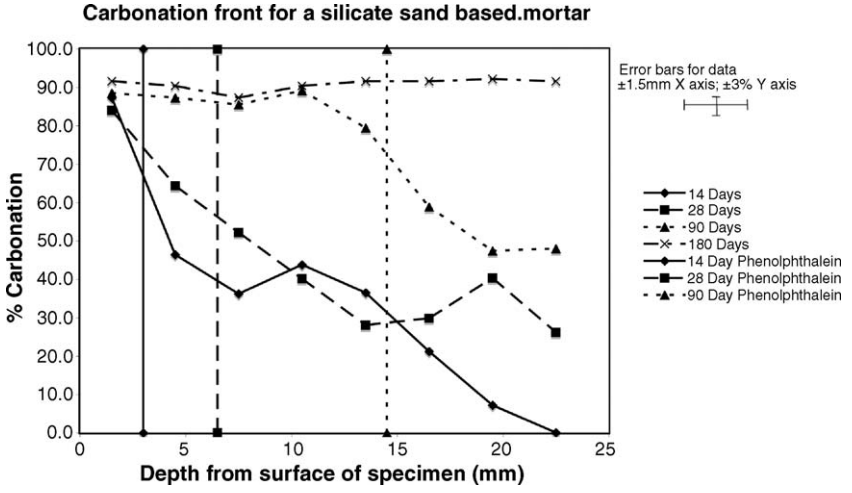

Fig. 8. Carbonation calculations for a lime mortar made with silicate sand.

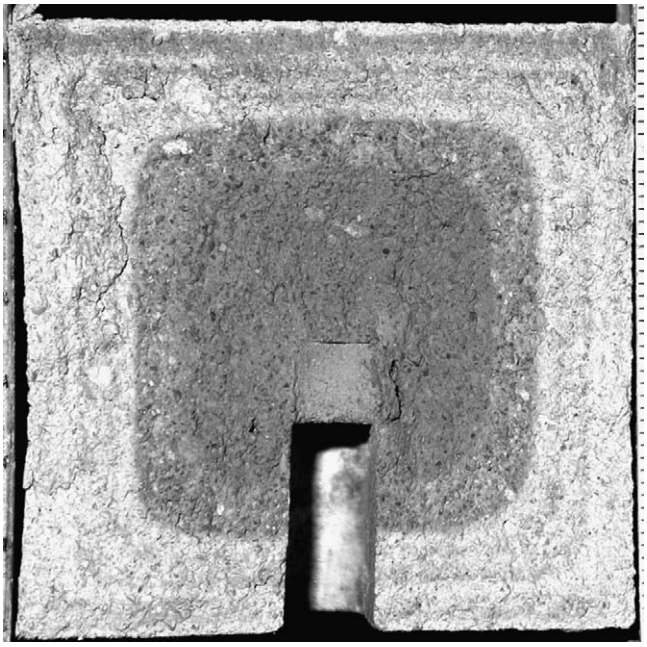

Fig. 9. Mortar surface a few seconds after spraying with phenolphthalein.

silicate sand mortar carbonates the most quickly as a result of this and the oolitic mortar carbonates the slowest.

Fig. 6 shows data for a lime mortar made with crushed oolitic limestone. The slope of each time interval curve is similar and relatively steep, going from maximum to minimum over a distance of about 5 mm.

Fig. 7 shows similar data for a lime mortar made with a crushed bioclastic limestone. The carbonation front gets steeper as time progresses, and the 180 day core carbonation develops to a greater extent than in the oolitic limestone.

Fig. 8 shows the data for a lime mortar made with a silicate sand. This shows a more extended carbonation front than that seen with the other mortars, a more rapid progression through the material and a more rapid growth of carbonation at the core.

The data at day 14 are unreliable at the chosen TGA resolution because the carbonation depth is significantly less than the resolution of the TGA data. Early tests on the sand mortars were compromised by the fact that in an agate mortar the sand was not crushed to a satisfactory fineness. This had the effect that TGA samples were not necessarily representative since they tended to contain lower proportions of aggregate compared with binder, as it was the finer material that tended to be collected by a spatula. This problem has subsequently been corrected by using a heavy cast iron pestle and mortar, which satisfactorily crushes the sand particles to the same size as the binder. It is probable that the 0% carbonation shown at the core of the 14 day sand sample is due to the errors inherent in the sampling technique at that time, since a small amount of carbonation would have been expected to be detected.

The percentage carbonation data at the depths indicated by phenolphthalein staining can be compared (Table 5) and it can be seen that at days 28 and 90 the phenolphthalein staining ceases to be apparent once carbonation has progressed beyond between 50% and 59%. The implication of this is that an unstained mortar could still contain between 40% and 50% uncarbonated lime.

Where the carbonation depth is on the cusp of two TGA measurements, a simple mean between the two measurements has been taken in order to better reflect the likely concentration of $Ca(OH)_2$ present. The resolution of the phenolphthalein data is 0.5 mm, whereas the resolution of the TGA data is 5 mm for the early data sets and 3 mm for later measurements. It is quite feasible to improve this resolution to 1 mm over ±3 mm of the phenolphthalein carbonation depth since this would only require an additional six tests. The resolution is limited not only by the aggregate size and the sample size but also by the friability of most lime mortars. Where a mortar is sufficiently dense and well cemented, greater resolution can be obtained. It has been shown that sampling at 0.2–0.5 mm intervals is possible in sand/cement mortars [20].

Fig. 9 shows a photograph of a 59 day-old specimen made with one part dry hydrate to three parts oolitic stone a few seconds after being sprayed with phenolphthalein. Fig. 10 shows the same surface 30 min after spraying. A phenomenon which is occasionally observed in lime mortars is the presence of Liesegang patterns. The Liesegang phenomenon is a quasi-periodic self-organised precipitation of a sparingly soluble product in the wake of a moving reaction front [21]. These are

Table 3
Open porosity of mortars as calculated by BSEN 1936:1999

	Bioclastic mortar	Oolitic mortar	Silicate sand mortar
Open porosity (%)	29.20	28.23	18.66

Table 4
Pore size distribution of mortars as measured by Mercury Intrusion Porosimetry

Intrusion volume (%)	Bioclastic mortar	Oolitic mortar	Silicate sand mortar
>10 μm	13.33	2.88	29.17
10 μm > 1 μm	11.12	10.81	2.54
1 μm > 0.1 μm	30.16	54.07	13.98
0.1 μm > 0.01 μm	21.50	18.99	23.19
<0.01 μm	23.89	13.25	31.12
Total	100	100	100

Table 5
Percentage carbonation as measured by TGA at phenolphthalein carbonation depth

Mortar filler type	Phenolphthalein carbonation depth (PCD) (mm)				$Ca(OH)_2$ at PCD per TGA (wt.%)					Carbonation at PCD per TGA (%)				
	Day 14	Day 28	Day 90	Day 180	Day 0	Day 14	Day 28	Day 90	Day 180	Day 0	Day 14	Day 28	Day 90	Day 180
Bioclastic	1.0	4.5	9.0	17.5	10.9	2.8	5.4	5.2	5.0	0.0	74.9	50.5	52.1	54.3
Oolitic	2.5	4.5	9.0	15.0	11.5	5.3	5.7	5.2	5.5	0.0	53.4	50.2	54.3	49.7
Sand	3.0	6.5	14.5	n/a	6.8	3.7	3.3	2.8	n/a	0.0	46.3	52.2	58.8	n/a
Mean											58.2	51.0	55.1	51.2
S.D.											14.9	1.1	3.4	3.2

characterised in lime mortars by concentric rings of stained and unstained material most often seen when the binder is an aged lime putty (>14 years old). The pale rings represent areas of mortar with a higher level of carbonation than the areas to either side. It can be seen that concentric Liesegang patterns which were initially visible have faded to the point of being barely detectable by eye after 30 min. The presence of a significant number of pores with a radius of <0.1 μm, due to the use of long-term aged lime with smaller $Ca(OH)_2$ crystals, has been suggested as being critical for the formation of Liesegang patterns [21]. Although the mortar under test was made with dry hydrated lime, the fine pore structure (Fig. 13) produced by the use of an oolitic filler would seem to produce the same result.

Fig. 11 shows the top right hand corner of Fig. 9 enlarged and visually enhanced.

The light stripes represent areas of lower concentrations of $Ca(OH)_2$. These are difficult to distinguish, but are approximately 3 mm, 5 mm, and a wider band at 7 mm from the exterior.

Fig. 12 shows a high resolution TGA analysis this specimen. Samples were taken at 0.67 mm intervals for the first 16 mm depth, followed by 3 mm intervals between 16 and 25 mm where the mortar showed no apparent carbonation. The graph shows

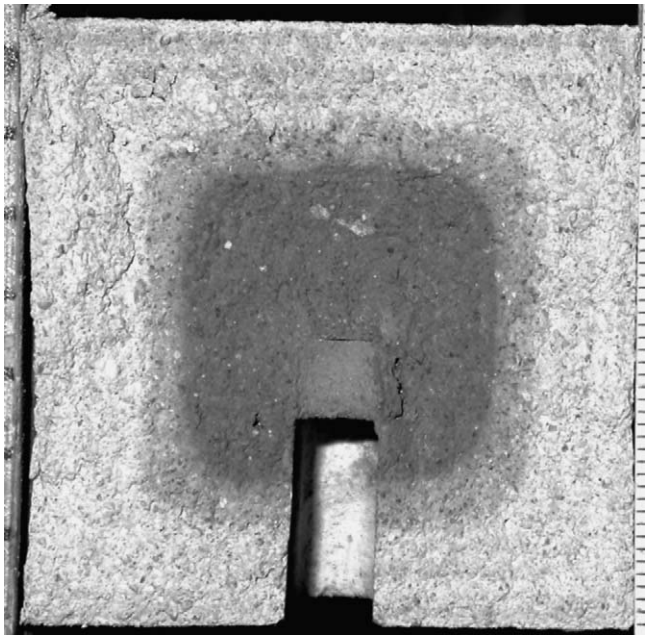

Fig. 10. Mortar surface 30 min after spraying with phenolphthalein.

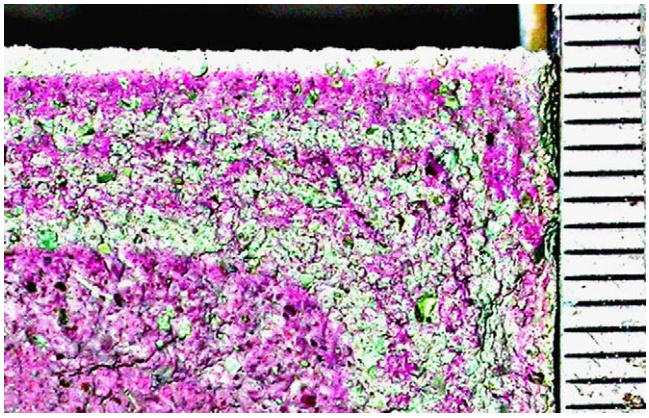

Fig. 11. Enhanced image of Liesegang patterns alternating stained and unstained regions seen on a specimen a few seconds after spraying with phenolphthalein. (Graticule to the right is for scale – each division represents 1 mm.)

the $Ca(OH)_2$ (%) as measured by TGA together with the calculated carbonation (%) superimposed on a scale photograph of the specimen. Error bars are shown to one side to make the graph easier to read. The error in the *X*-axis is ±0.33 mm, and in the *Y*-axis ±2% as established by repeat testing of three different samples at this resolution. The presence of Liesegang patterns is shown by vertical dotted lines (thick lines for wide patterns, and thin lines for narrow patterns). It can be seen that the oscillations in the $Ca(OH)_2$ (%) coincide with the presence of the Liesegang patterns.

Fig. 12 clearly demonstrates that the change from carbonated to uncarbonated is not a sudden transition, but rather a steady change with periodic oscillations. While the colour changes in the phenolphthalein are difficult to define clearly it would seem that these oscillations are coincident with the presence of Liesegang patterns. This is a phenomenon, which requires further research.

4. Discussion

4.1. Comparison with phenolphthalein staining

In spite of the difference in resolution between the phenolphthalein staining data and the TGA data, it is evident that it is erroneous to assume that a material, which is not stained by phenolphthalein has fully carbonated. The TGA data demonstrates that between 40% and 50% of the binder has still to carbonate at the boundary between unstained and stained material.

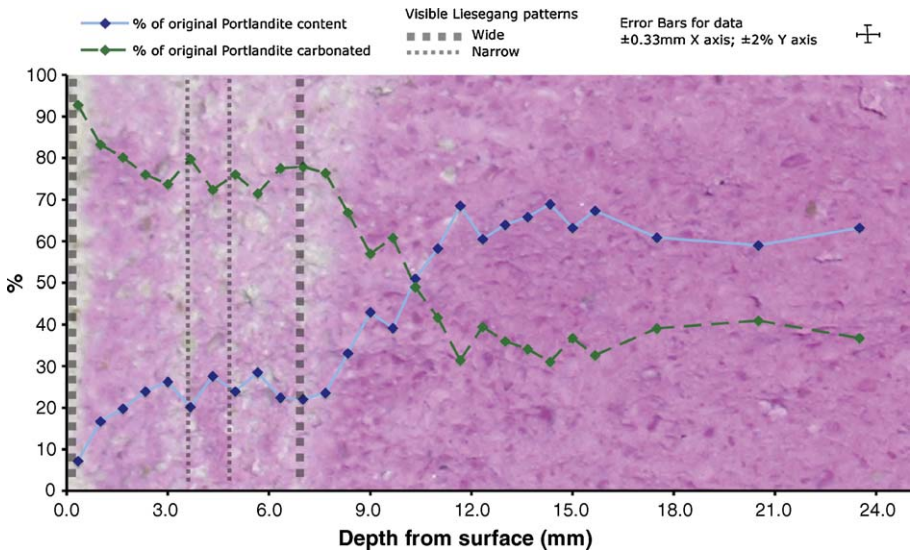

Fig. 12. High resolution TGA profile of a 59 day-old lime/oolitic stone mortar (intervals of 0.67 mm). % $Ca(OH)_2$ TGA readings and calculated % carbonation are superimposed on a scale photograph of a freshly phenolphthalein stained surface.

The phenolphthalein staining depth appears to fall consistently half way between the start and the finish of the carbonation front. This demonstrates that phenolphthalein staining is a reliable and consistent method of measuring the average depth of carbonation. The major caveat to be accepted by practitioners is that the phenolphthalein staining depth is not a true indication of the extent of carbonation. It cannot be assumed that unstained material is fully carbonated, nor that stained material is completely uncarbonated.

Since Liesegang patterns are of the order of 1 mm in thickness, as has been demonstrated, TGA can be used to investigate this phenomenon by identifying the extent of any differences in carbonation.

4.2. Comparison with average TGA measurements

Analysis of carbonation of lime mortars by TGA is often done by taking an average of the readings from a sample taken from the exterior of a specimen and a sample taken from the core [22,23], or the mean of three measurements [24]. In other cases the sampling method is not described, but only one measurement at each time-frame is reported [25,26]. The resulting reading is compared with results taken at different times in the carbonation process in order to map the progress of carbonation.

As can be seen from the data in Figs. 6–8, this can produce a misleading result since the technique assumes a straight line progression between the ‘carbonated’ exterior and the ‘uncarbonated’ core, which is not the case.

Where a sample is taken through the entire cross-section from exterior to core, a more representative average can be produced. Great care must be taken in sampling using this technique. Since the sample under test is ∼50 mg, if the cross-sectional sample is much greater than this, there is a risk that the sample tested might not be truly representative of the average. This was an error that was encountered in early tests [27] where the sample taken was ∼3 g. Accuracy was much improved when this sample size was reduced to ∼0.25 g.

The use of an ‘average’ carbonation figure is also misleading because it ignores the fact that carbonation progresses from the exterior towards the core. When comparing one younger specimen with another identical older specimen, an average result can give an indication of the progression of carbonation. This is not easily comparable with a specimen made with a different mix or type of lime. The only valid technique for comparing extents of carbonation between specimens is by looking at either the depth of carbonation or preferably the shape and position of the carbonation front.

4.3. The shape of the carbonation front

The following conclusions can be drawn from the TGA data:

- The silicate sand mortar carbonates to a greater extent than the other two mortar mixes. It achieves ∼88% carbonation compared with ∼82% for the other two mortars at 90 days. By 180 days the silicate sand mortar appears to have completed its carbonation process, at an average of ∼91%.
- The silicate sand mortar carbonates more quickly than the other two mortars. The start of the carbonation front is at ∼12 mm at 90 days, compared with ∼8 mm for the other mortars. By 180 days full carbonation appears to have occurred in the silicate sand mortar, while there is still 5–7.5 mm of material yet to fully carbonate in the other mortars.
- The carbonation front in the silicate sand mortar extends over a greater distance than the other two mortars. The extent is ∼10 mm compared with ∼5 mm for oolitic and ∼7.5 mm for bioclastic. This is likely to be related to the pore size distribution, particularly to the amount of pores present that are >10 μm.
- The core of the silicate sand mortar carbonates ahead of the carbonation front at a faster rate than the other two mortars.

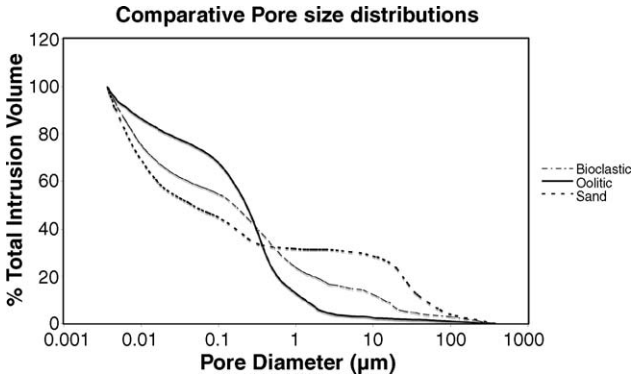

Fig. 13. Total intrusion volume (%) as measured by Mercury Intrusion Porosimetry.

~48% carbonation was achieved after 90 days compared with ~19% for oolitic and ~13% for bioclastic. The core of the oolitic mortar appears to remain relatively uncarbonated even at 180 days, whereas the bioclastic mortar is showing signs of increasing carbonation.

- The slope of the carbonation front of the silicate sand mortar is similar at all time intervals, as it is with the oolitic mortar. The bioclastic mortar shows an increase in the gradient of the carbonation front with up to 90 days, although the gradient reduces at 180 days. The increase in gradient seen in the bioclastic mortar might be associated with pore blocking caused by a pozzolanic reaction which has been identified in this mortar [26]. Such pore blocking would reduce the accessibility of CO_2 to the interior, and hence inhibit carbonation.

The increased rate and extent of carbonation seen in the silicate sand mortar when compared with the other two mortars is likely to be due to larger pore sizes present in this material since the sand contained <20% fines (<63 μm) compared with ~30% for the bioclastic and ~40% for the oolitic. This would allow easier passage of CO_2 towards the core of the material. Fig. 13 shows the relative pore sizes as measured by Mercury Intrusion Porosimetry. It can be seen that the pores in the oolitic mortar are mainly below 1 μm in diameter whereas there are significant quantities of larger pores in the sand mortar, with the bioclastic mortar falling somewhere in between.

The observed difference in maximum carbonation achieved between the mortars with crushed stone filler and the mortar with silicate sand filler is unlikely to be a result of pore size reduction limiting access to CO_2 [28] since, once the maximum carbonation level is achieved, it is independent of the depth from the surface. It is more likely that portlandite particles tend to become enclosed by an impervious shell of calcite [29,30], which effectively prevents complete carbonation. Studies of medieval mortars have revealed the continuing presence of residual portlandite [31], demonstrating that this phenomenon can be long lasting.

4.4. Implications of the proposed system

As the sampling technique employed arrests the carbonation process, TGA testing can be conducted up to 41 days after sampling takes place [17] without affecting the result. This also means that a much higher resolution map of the carbonation front could be conducted over the entire specimen depth over a period of no more than 3 days. (The testing technique employed requires approximately 45 min per sample, thus at 1 mm resolution a full 25 mm profile could be produced in around 19 h.) This would be particularly interesting in an investigation of the way in which carbonation develops at the core of the specimen.

Care should be taken before applying this technique to the measurement of carbonation in hydraulic limes. The amount of $Ca(OH)_2$ measured by TGA is understated when in the presence of calcium silicate hydrates [32], and further work is required to validate the technique in such circumstances.

4.5. Errors and inconsistencies in the data

During the course of these experiments the technique has been sophisticated in a number of ways in order to reduce errors and inconsistencies as they became apparent.

- Sample depth has been reduced from 5 mm to 3.0–0.67 mm. The smaller the sample interval, the greater the resolution capable of being achieved. A compromise needs to be struck between resolution and available machine time, but it is suggested that a maximum sample depth of 2 mm should be used, reducing to 1 mm where time and resources are available.
- Great care needs to be taken to grind all of the material sampled down to ~60 μm. Where hard fillers are present suitable techniques should be applied to crush these to a similar fineness as the binder. This is necessary in order to consistently and reproducibly measure the wt.% of binder present not only between distance intervals but also between mortars tested at different times.
- In some cases it can be seen that the carbonation (%) does not decrease consistently through the depth of the mortars. For example the 14 day sand mortar shows higher carbonation at 10 mm than at 5 mm and the 28 day sand mortars shows higher carbonation at 20 mm than at 15 mm. This is unlikely to be due to inaccuracies in the measuring technique. A large number of calibration tests have been conducted demonstrating the accuracy of the technique, so any differences seen are more likely to be real rather than the result of experimental error. Such differences may either be due to inhomogeneity in the mortar, or to the presence of oscillations in the level of carbonation such as are seen in Liesegang patterns and as demonstrated in Fig. 9 above.

5. Conclusions

The use of TGA on depth profiles of lime mortars provides a greater insight into the progression of carbonation than traditional methods can offer. The three mortars under study show very different carbonation profiles, which would not be apparent using either phenolphthalein staining or by taking an average TGA measurement.

Apart from demonstrating the validity of the technique, and the possibility of producing more detailed profiles, four other insights of significance have been gained:

1. The carbonation front does not necessarily progress through the mortar in a linear manner. Under certain circumstances the slope of the carbonation front can change in steepness.
2. The carbonation front demonstrates oscillations coincident with the presence of Liesegang patterns, and it might be that such oscillations are characteristic of the carbonation process.
3. A small amount of carbonation occurs at the core of the mortar ahead of the carbonation front, at a rate which is likely to be related to the pore size distribution of the mortar.
4. Even when the carbonation process has apparently run its course, lime mortars still retain a significant amount of uncarbonated lime.

References

[1] O. Cazalla, C. Rodriguez-Navarro, E. Sebastian, G. Cultrone, M.J. De La Torre, J. Am. Ceram. Soc. 83 (2000) 1070–1076.
[2] B. Johannesson, P. Utgenannt, Cem. Concr. Res. 31 (2001) 925–931.
[3] M. Arandigoyen, J.L. Pérez Bernal, M.A. Bello López, J.I. Alvarez, Appl. Surf. Sci. 252 (2005) 1449–1459.
[4] R.M.H. Lawrence, Proceedings of the International Building Lime Symposium, Orlando, 2005.
[5] D.R. Moorehead, Cem. Concr. Res. 16 (1986) 700–708.
[6] R.M.H. Lawrence, T.J. Mays, P. Walker, D. D'Ayala, J. Therm. Anal. Cal. doi:10.1007/s10973-005-7302-7.
[7] British Standards, BS EN 1015-3, 1999.
[8] A.M. Neville, Properties of Concrete, Longman, Harlow, 1995.
[9] G. Allen, J. Allen, N. Elton, M. Farey, S. Holmes, P. Livesey, M. Radonjic, Hydraulic Lime Mortar for Stone, Brick and Block Masonry, Donhead Publishing, Shaftesbury, 2003.
[10] J. Lanas, J.I. Alvarez-Galindo, Cem. Concr. Res. 33 (2003) 1867–1876.
[11] Y.F. Houst, F.H. Wittmann, Cem. Concr. Res. 32 (2002) 1923–1930.
[12] J.M. Teutonico, I. McCraig, C. Burns, J. Ashurst, Bull. Assoc. Preserv. Technol. 25 (1994) 32–49.
[13] British Standards, BS EN 1015-11, 1999.
[14] P. Bromblet, Int. J. Restoration Build. Monuments 6 (2000) 513–528.
[15] J. Stewart, R. Glover, J. Houston, N. Seeley, T. Proudfoot, J. Architectural Conserv. 7 (2001) 7–41.
[16] G. Baronio, L. Binda, A. Saisi, in: P. Bartos, C. Groot, J.J. Hughes (Eds.), International RILEM Workshop on Historic Mortars: Characteristics and Tests, RILEM Publications, 2000, pp. 307–325.
[17] R.M. Dheilly, J. Tudo, Y. Sebai bi, M. Queneudec, Construct. Build. Mater. 16 (2002) 155–161.
[18] K. Przepiera, J. Therm. Anal. Cal. 74 (2003) 659–666.
[19] British Standards, BSEN 1936, 1999.
[20] J.J. Thomas, J. Hsieh, H.M. Jennings, Adv. Cem. Bas. Mater. 3 (1996) 76–80.
[21] C. Rogriguez-Navarro, O. Cazalla, K. Elert, E. Sebastian, Proc. R. Soc. Lond. A 458 (2002) 2261–2273.
[22] J. Lanas, J.L. Perez Bernal, M.A. Bello, J.I. Alvarez, Cem. Concr. Res. 34 (2004) 2191–2201.
[23] J. Lanas, R. Sirera, J.I. Alvarez, Thermochim. Acta 429 (2005) 219–226.
[24] A. Moropoulou, A. Bakolas, E. Moundoulas, E. Aggelakopoulou, S. Anagnostopoulou, Cem. Concr. Comp. 27 (2005) 289–294.
[25] A. Bakolas, A. Biscontin, A. Moropoulou, E. Zendri, Thermochim. Acta 321 (1998) 151–160.
[26] A. Moropoulou, A. Bakolas, E. Aggelakapoulou, Thermochim. Acta 420 (2005) 135–140.
[27] R.M.H. Lawrence, D. D'Ayala, P. Walker, J. Architectural Conserv. 12 (March) (2006) 7–33.
[28] G. Cultrone, E. Sebastian, M. Ortega Huertas, Cem. Concr. Res. (2006).
[29] K. Van Balen, Cem. Concr. Res. 35 (2005) 647–657.
[30] R.M. Dheilly, J. Tudo, M. Queneudec, J. Mater. Eng. Perform. 7 (1998) 780–795.
[31] J. Adams, D. Dollimore, L.D. Griffiths, Thermochim. Acta 324 (1988) 67–76.
[32] G.L. Valenti, R. Cioffi, J. Mater. Sci. Lett. 4 (1985) 475–478.